ELSEVIER

Journal of Nuclear Materials 290–293 (2001) 609–614

journal of nuclear materials

www.elsevier.nl/locate/jnucmat

Calculation of 2D profiles for the plasma and electric field in the boundary layer of the TEXTOR-94 Tokamak

H. Gerhauser [a,*], R. Zagórski [b], H.A. Claaßen [a], M. Lehnen [a]

[a] Institut für Plasmaphysik, Forschungszentrum Jülich GmbH, EURATOM Association, Trilateral Euregio Cluster, D-52425 Jülich, Germany

[b] Institute of Plasma Physics and Laser Microfusion, 23 Hery Street, P.O. Box 49, 00-908 Warsaw, Poland

Abstract

An improved version of the 2D multifluid code TECXY is used to study the plasma parameters and the electric field in the boundary layer of the TEXTOR-94 tokamak. An anomalous perpendicular shear viscosity $\eta_\perp$ is incorporated into the ion momentum balance which allows to fulfil the global (magnetic surface averaged) ambipolarity constraint for the radial electric current, and to determine the electric field in the transition layer by a second-order ordinary differential equation for $E_r(r)$. The code modelling results suggest the existence of a narrow global circulation layer for the poloidal plasma velocity just inside the separatrix which is connected with a negative electric field spike. A proper choice of $\eta_\perp$ gives better agreement with experimental velocity profiles.

Keywords: 2D fluid code; Plasma edge; Radial electric field; TEXTOR; Modelling

1. Introduction

The 2D boundary layer code TECXY [1–4] has been proved to be a useful tool for investigating specific physical questions in the plasma edge of limiter tokamaks. The physical model is based on Braginskij-like equations. Moreover the present version of the code incorporates drift motions and currents in a fully self-consistent way with plasma and impurity dynamics.

In this paper, we use an improved version of TECXY to study the plasma parameters and the electric field in the boundary layer of the TEXTOR-94 tokamak. The code improvements concern the correct formulation of the anomalous transport in the electron/ion energy balance and the incorporation of anomalous shear viscosity effects (first proposed in [5]) in the ion momentum balance. The hitherto assumed radial profile shape of the rotational ion drift velocity inside the separatrix has now been replaced by a calculated one, based on the global ambipolarity constraint. The latter originally formulated for the revisited nc theory [6] has been modified to apply also to turbulent (L-mode) plasmas [7].

Simulations with the TECXY transport code illustrate the influence of drifts on the plasma flows near the separatrix. The significance of different physical mechanisms for the potential profile and the resulting electric field is studied in detail. Recent measurements of the poloidal velocity profile [8] are in good agreement with the code modelling which suggests the existence of a narrow global circulation layer just inside the separatrix. Such a layer had first been conjectured in [9], but the present more refined calculations show that the width of this global circulation layer is only about 1 cm.

2. Physical model

The 2D boundary layer code TECXY [1,2,4] is primarily based on the classical transport equations derived by Braginskij [10]. The transport along field lines is assumed to be classical [11], whereas the radial transport is assumed to be anomalous with prescribed radial transport coefficients of the order of Bohm diffusion. The

* Corresponding author. Tel.: +49-2461 61 5648; fax: +49-2461 61 2970.

E-mail address: h.gerhauser@fz-juelich.de (H. Gerhauser).

PII: S 0 0 2 2 - 3 1 1 5 (0 0) 0 0 6 0 2 - 4

dynamics of deuterium and impurity neutrals in the SOL is described by an analytical model, which accounts in a self-consistent way for recycling of plasma ions as well as for sputtering processes at the limiter plates.

2.1. Multifluid equations

For every ion species a ($a = i$ for deuterium ions and $a = j$ for the different charge states of impurity ions) we solve the continuity, parallel momentum and energy equations. The continuity equation contains the source S_n^a from ionization of neutrals. The equation of motion is:

$$n_a m_a \frac{\partial \overrightarrow{V_a}}{\partial t} + n_a m_a \overrightarrow{V_a} \cdot \nabla \overrightarrow{V_a} + \mathrm{div} \overleftrightarrow{\Pi}_a = -\nabla p_a + n_a e_a \left(\vec{E} + \overrightarrow{V_a} \times \vec{B} \right) + \overrightarrow{R_a} + \left(\overrightarrow{S_V^a} - m_a \overrightarrow{V_a} S_n^a \right), \quad (1)$$

where $\overrightarrow{R_a} \equiv \overrightarrow{R_V^a} + \overrightarrow{R_T^a}$ are friction and thermal forces, $\overrightarrow{S_V^a}$ the sources (sinks) of momentum, p_a the pressure and $\overleftrightarrow{\Pi}_a$ is the viscosity tensor. For the energy balance equations we refer to [4].

We use coordinates x, y and z corresponding to the poloidal, radial and toroidal directions, respectively. Note that $\sqrt{g} = h_x h_y h_z = h_\perp h_y h_\parallel$ is the product of metric coefficients, whereas $b_x = -B_\Theta/B$ and $b_z = B_\phi/B$ are magnetic field ratios.

According to Braginskij [10], the viscosity tensor $\overleftrightarrow{\Pi}$ can be expressed as: $\overleftrightarrow{\Pi} = -\sum_i \eta_i \overleftrightarrow{W}_i$, $i = 0$ to 4, where η_3 and η_4 refer to gyroviscosity and will not be treated here. η_0 is the classical parallel viscosity, and $\overleftrightarrow{W}_0$ is related to the rate-of-strain tensor.

In the coordinate system $(\parallel, \perp, y)$ the classical part $\overleftrightarrow{\Pi}^{\mathrm{cl}}$ of the viscosity tensor is purely diagonal:

$$\Pi^{\mathrm{cl}}_{\parallel\parallel} = -\eta_0 W_{\parallel\parallel} \equiv 2b, \quad \Pi^{\mathrm{cl}}_{yy} = \Pi^{\mathrm{cl}}_{\perp\perp} = \frac{1}{2}\eta_0 W_{\parallel\parallel} = -b$$

with

$$W_{\parallel\parallel} = \frac{2}{h_\parallel}\frac{\partial V_\parallel}{\partial x_\parallel} + 2\left(\vec{V} \cdot \nabla - \frac{V_\parallel \partial}{h_\parallel \partial x_\parallel} \right) \ln h_\parallel - \frac{2}{3}\,\mathrm{div}\,\vec{V}. \quad (2)$$

In the following we will neglect derivatives of the logarithm of metric coefficients in all viscosity terms. Furthermore we will assume a tokamak ordering for plasma velocities: $b_z \sim 1, b_x = \varepsilon \sim 0.1, V_\theta \sim V_\perp \sim \varepsilon V_\parallel, V_y \sim \varepsilon^2 V_\perp \sim \varepsilon^3 V_\parallel$, $\partial V/\partial x \sim \varepsilon^2 \partial V/\partial y$. Thus $W_{\parallel\parallel}$ simplifies to

$$W_{\parallel\parallel} = \frac{4}{3}\left(\frac{b_x}{h_x}\frac{\partial V_\parallel}{\partial x} - \Omega \right) \quad \text{with}$$

$$\Omega = \frac{1}{2}\left(\frac{b_z}{h_x}\frac{\partial V_\perp}{\partial x} + \frac{1}{h_y}\frac{\partial V_y}{\partial y} \right).$$

The coefficients $\eta_2 = \eta_y$ and $\eta_1 = \eta_\perp = (1/4)\eta_y$ describe the shear viscosity and, like in [5], are assumed to be anomalously enhanced, so that the leading terms of $\overleftrightarrow{\Pi}_a^{an}$ are:

$$\Pi^{an}_{\parallel y} = \Pi^{an}_{y\parallel} = -\eta_y \frac{1}{h_y}\frac{\partial V_\parallel}{\partial y}, \quad \Pi^{an}_{\perp y} = \Pi^{an}_{y\perp} = -\eta_\perp \frac{1}{h_y}\frac{\partial V_\perp}{\partial y}.$$

Using $\eta_x = (4/3)\eta_0 b_x^2$ we get the parallel component of the momentum equation in the final form:

$$m_a n_a \frac{\partial V_{a\parallel}}{\partial t} + m_a n_a \left[\left(\frac{V_{ax}}{h_x}\frac{\partial}{\partial x} + \frac{V_{ay}}{h_y}\frac{\partial}{\partial y} \right) V_{a\parallel} + b_z V_{a\parallel} V_{a\perp} \frac{1}{h_x}\frac{\partial}{\partial x} \ln(h_z b_z) \right] - \frac{1}{\sqrt{g}}\frac{\partial}{\partial x}\frac{\sqrt{g}}{h_x^2}\eta_x^a \frac{\partial V_{a\parallel}}{\partial x} - \frac{1}{\sqrt{g}}\frac{\partial}{\partial y}\frac{\sqrt{g}}{h_y^2}\eta_y^a \frac{\partial V_{a\parallel}}{\partial y} + \frac{1}{\sqrt{g}}\frac{\partial}{\partial x}\left(\frac{\sqrt{g}}{h_x b_x}\eta_x^a \Omega_a \right) = -\frac{b_x}{h_x}\left(\frac{\partial p_a}{\partial x} + \frac{e_a n_a}{e n_e}\frac{\partial p_e}{\partial x} \right) + R_{a\parallel} + \frac{e_a n_a}{e n_e} R_{e\parallel} + \left(S^a_{V_\parallel} - m_a V_{a\parallel} S_n^a \right) \quad (3)$$

2.2. Drifts and currents

In order to consider drift motions and currents, additional equations are obtained from the diamagnetic and radial components of Ohm's law and the equation of motion. We have perpendicular drift velocities and, in addition to the radial diffusion velocities $-D_y^a \partial \ln n_a / h_y \partial y$, also radial drift velocities:

$$V_{a\perp} = \frac{1}{e_a n_a B}\frac{1}{h_y}\left[-\frac{\partial}{\partial y}(p_a - b_a) - e_a n_a \frac{\partial \Phi}{\partial y} + \left(3b_a + m_a n_a V_{a\parallel}^2 \right)\frac{\partial}{\partial y}\ln(h_z b_z) \right], \quad (4)$$

$$V^d_{ay} = \frac{1}{e_a n_a B}\left[\frac{B}{h_x h_z}\frac{\partial}{\partial x}\left(\frac{h_z b_z}{B}(p_a - b_a) \right) + e_a n_a \frac{b_z}{h_x}\frac{\partial \Phi}{\partial x} - \left(2p_a + b_a + m_a n_a V_{a\parallel}^2 \right)\frac{b_z}{h_x}\frac{\partial}{\partial x}\ln(h_z b_z) + m_a n_a \overrightarrow{V_a} \cdot \nabla V_{a\perp} - \left(S^a_{V\perp} - m_a V_{a\perp} S^a_n \right) - \frac{1}{\sqrt{g}}\frac{\partial}{\partial y}\frac{\sqrt{g}}{h_y^2}\eta^a_\perp \frac{\partial V_{a\perp}}{\partial y} \right], \quad (5)$$

$$V_{e\perp} = \frac{1}{B h_y}\left[\frac{1}{e n_e}\frac{\partial p_e}{\partial y} - \frac{\partial \Phi}{\partial y} \right], \quad V^d_{\mathrm{ey}} = \frac{-b_z}{B h_x}\left(\frac{1}{e n_e}\frac{\partial p_e}{\partial x} - \frac{\partial \Phi}{\partial x} \right). \quad (6)$$

The diamagnetic and radial components of the plasma current are derived from Eqs. (4)–(6):

$$j_\perp = -\frac{1}{B}\left[\frac{\partial}{\partial y}\left(p - \sum_a b_a\right) - \sum_a \left(3b_a + m_a n_a V_{a\|}^2\right) \times \frac{1}{h_y}\frac{\partial}{\partial y}(h_z b_z)\right], \quad (7)$$

$$j_y = \frac{b_z}{Bh_x}\left[\frac{B}{b_z h_z}\frac{\partial}{\partial x}\left(\frac{h_z b_z}{B}\left(p - \sum_a b_a\right)\right) - \left(2p + \sum_a b_a + m_a n_a V_{a\|}^2\right)\frac{\partial}{\partial x}\ln(h_z b_z)\right] + \frac{1}{B} \times \left[\sum_a m_a n_a \vec{V_a}\cdot\nabla V_{a\perp} - \sum_a\left(S^a_{V_\perp} - m_a V_{a\perp} S^a_n\right) - \sum_a \frac{1}{\sqrt{g}}\frac{\partial}{\partial y}\frac{\sqrt{g}}{h_y^2}\eta^a_\perp \frac{\partial V_{a\perp}}{\partial y}\right]. \quad (8)$$

The essential new term in the radial drift velocity V^d_{ay} (and current j_y) is related to the force from the perpendicular shear viscosity $\eta^a_\perp$. It may be of the same order as the competing forces, namely the Lorentz force, the ∇B and centrifugal forces and the forces from inertia and momentum transfer from neutrals.

The poloidal component of the plasma current can be expressed by the parallel and perpendicular components: $j_x = b_x j_\| + b_z j_\perp$. Using Kirchhoff's law

$$\mathrm{div}\ \vec{j} = \frac{1}{\sqrt{g}}\left(\frac{\partial}{\partial x}\frac{\sqrt{g}}{h_x}j_x + \frac{\partial}{\partial y}\frac{\sqrt{g}}{h_y}j_y\right) = 0,$$

we can introduce the stream function $\Psi(x,y)$ by $\sqrt{g}j_x/h_x = -\partial\Psi/\partial y$ and $\sqrt{g}j_y/h_y = \partial\Psi/\partial x$. It is determined up to some function of y: $\Psi(x,y) = \widetilde{\Psi}(x,y) + F(y) = \int_{x_p}(\sqrt{g}j_y/h_y)\,\mathrm{d}x + F(y)$. Hence the poloidal and parallel components of the current are: $j_x = \widetilde{j}_x + j_{xc} \equiv -(h_x/\sqrt{g})(\partial\widetilde{\Psi}/\partial y + \mathrm{d}F/\mathrm{d}y)$ and similarly $j_\| = \widetilde{j}_\| + j_{\|c} = (\widetilde{j}_x - b_z j_\perp)/b_x + j_{xc}/b_x$.

$F(y)$ can now be determined from the condition for a unique electrostatic potential:

$$\int_{x_{\mathrm{is}}}^{x_{\mathrm{es}}}\left(\frac{\partial\Phi_0}{\partial x} - \frac{h_x}{b_x}\frac{j_\|}{\sigma_\|}\right)\mathrm{d}x = \int_{x_{\mathrm{is}}}^{x_{\mathrm{es}}}\left(\frac{1}{en_e}\frac{\partial p_e}{\partial x} + \frac{\alpha_T}{e}\frac{\partial T_e}{\partial x} - \frac{h_x}{b_x}\frac{j_\|}{\sigma_\|}\right)\mathrm{d}x = \Delta\Phi_{\mathrm{es}} - \Delta\Phi_{\mathrm{is}}. \quad (9)$$

Thus

$$F' \equiv \frac{\mathrm{d}F}{\mathrm{d}y} = \frac{(\Delta\Phi_{\mathrm{es}} - \Phi_{0\mathrm{es}}) - (\Delta\Phi_{\mathrm{is}} - \Phi_{0\mathrm{is}}) + \int_{x_{\mathrm{is}}}^{x_{\mathrm{es}}}\mathrm{d}x\,(h_x/b_x)\widetilde{j}_\|/\sigma_\|}{\int_{x_{\mathrm{is}}}^{x_{\mathrm{es}}}\mathrm{d}x\,h_x^2/(b_x^2\sigma_\|\sqrt{g})}. \quad (10)$$

The potential drop in the Langmuir sheath $\Delta\Phi \geqslant 0$ is given by $\Delta\Phi = \Delta\Phi^{\mathrm{sh}} - T_e/e\ln(1 - j_x/\sum_a e_a n_a V_{ax})$, where $\Delta\Phi^{\mathrm{sh}}(\sim 3T_e/e)$ is the drop without poloidal current. Since $j_x = \widetilde{j}_x - h_x F'/\sqrt{g}$ the equation for F' is strongly nonlinear in the scrape-off layer (SOL), but there the function F' uniquely determines potential and currents. However, in the transition layer, where $\Delta\Phi = 0$, the potential at one line (e.g., bisectrix) has to be given in order to close the system of equations.

2.3. Equation for the radial electric field

The global ambipolarity on closed magnetic surfaces means: $\langle j_y\rangle \equiv \oint_x j_y h_z h_x\,\mathrm{d}x = 0$, or

$$0 = \oint h_z h_x\left(-\frac{1}{B}\frac{b_z}{h_x}\left[\left(2p + \sum_a\left(b_a + m_a n_a V_{a\|}^2\right)\right)\times\frac{\partial}{\partial x}\ln(h_z b_z)\right] - \frac{1}{B}\sum_a m_a c^a_s b_x P^a_2\right)\mathrm{d}x + \oint h_z h_x\left[\frac{1}{B}\sum_a m_a V_{a\perp}(P^a_1 + S^a_n) + \frac{1}{B}\sum_a m_a n_a\left(V_{ax}\frac{1}{h_x}\frac{\partial}{\partial x} + V_{ay}\frac{1}{h_y}\frac{\partial}{\partial y}\right)V_{a\perp}\right]\mathrm{d}x - \oint h_z h_x\left(\frac{1}{B}\frac{1}{\sqrt{g}}\frac{\partial}{\partial y}\frac{\sqrt{g}}{h_y^2}\sum_a \eta^a_\perp\frac{\partial V_{a\perp}}{\partial y}\right)\mathrm{d}x \quad (11)$$

depending linearly on $V_{a\perp}$. The source term from the momentum transfer by cx with neutrals has been written as: $S^a_{V\perp} \equiv -m_a V_{a\perp}P^a_1 + m_a c^a_s b_x P^a_2$, where c^a_s is the sound speed, and P^a_1, P^a_2 are given.

Let us denote $\Phi = \Phi^* + \widetilde{\Phi}$, where $\Phi^* = \Phi^*(y) = \Phi(x_{\mathrm{bis}}, y)$ and $\widetilde{\Phi} = \widetilde{\Phi}(x,y)$ with $\widetilde{\Phi}(x_{\mathrm{bis}}, y) \equiv 0$. The condition for a unique electric potential $\oint\mathrm{d}\Phi = \oint\partial\Phi/\partial x\,\mathrm{d}x = \oint\partial\widetilde{\Phi}/\partial x\,\mathrm{d}x = 0$ means that $\widetilde{\Phi}(x,y)$ can be found for every y by integrating the parallel Ohm's law along x. At the separatrix Φ^* and $(\partial\Phi^*/\partial y)$ are given by the values obtained in the SOL. At the core boundary we use the condition, that the total poloidally circulating ion current from perpendicular ion motion vanishes: $\oint\sqrt{g}b_z j_{i\perp}\,\mathrm{d}x|_{y=0} = \oint\sqrt{g}b_z\sum_a e_a n_a V_{a\perp}\,\mathrm{d}x|_{y=0} = 0$, which yields $\mathrm{d}\Phi^*/\mathrm{d}y\,|_{y=0}$.

In the following we consider all quantities including $V_y, V_x, V_\|$ as given. Eq. (4) is expressed in terms of the unknown radial electric field by $V_{a\perp} = (G_a - (\partial\Phi^*/\partial y))/Bh_y$, where

$$G_a = \frac{1}{e_a n_a}\left[-\frac{\partial}{\partial y}(p_a - b_a) + \left(3b_a + m_a n_a V_{a\|}^2\right)\times\frac{\partial}{\partial y}\ln(h_z b_z)\right] - \frac{\partial\widetilde{\Phi}}{\partial y}. \quad (12)$$

Now, the ambipolarity constraint Eq. (11) is easily transformed into a linear differential equation of third order for Φ^* (second-order for $\mathrm{d}\Phi^*/\mathrm{d}y$):

$$B(y)\frac{\mathrm{d}\Phi^*}{\mathrm{d}y} + C(y)\frac{\mathrm{d}^2\Phi^*}{\mathrm{d}y^2} + D(y)\frac{\mathrm{d}^3\Phi^*}{\mathrm{d}y^3} = A(y), \qquad (13)$$

where $A(y)$, $B(y)$, $C(y)$ and $D(y) = -\oint \mathrm{d}x(h_x h_z/B^2 h_y^3) \sum_a \eta_\perp^a$ are known functions of the plasma parameters. The numerical solution of the differential equation is incorporated into the iteration loop for determining the drift quantities.

3. Results of calculations and discussion

We used standard boundary conditions in our calculations. The computational domain extends poloidally from one limiter side to the other limiter side and radially from $r = 42$ to $r = 50$ cm with the separatrix at $a = 46$ cm. At the core boundary a total power input and a total particle input flux are specified. At the wall we have used decay lengths as boundary conditions. At the limiter $V_x^a = \pm b_x c_s$ for the momentum equations and $q_x^e = \delta_e n_e V_x^e T_e$, $q_x^a = \delta_a n_a V_x^a T_i$ for the energy equations. At the auxiliary boundary, which continues the limiter sides into the transition layer, we have assumed that all quantities are continuous and poloidally periodic.

We performed calculations with the TECXY code for a high density auxiliary heated TEXTOR-94 discharge in deuterium but still neglected the effect of impurities. The belt limiter ALT-II is at $\theta = -45°$ position, the total magnetic field $B = 2.25$ T, the plasma current $I_\mathrm{p} = 350$ kA and the Shafranov shift $\Delta = 6$ cm. The anomalous transport in radial direction is determined by the coefficients $D_y = 1.5$ m^2/s, $\eta_y = \frac{1}{3} m_i n_i D_y$ and $\chi_y^e/n_e = \frac{3}{2}\chi_y^i/n_a = 2D_y$. For the present case the input particle flux to the SOL was $\Gamma_\mathrm{inp} = 5.5 \times 10^{21}$ s^{-1} and the power input $Q_\mathrm{inp} = 1$ MW. The recycling coefficient (the fraction of recycled neutrals reionized in the boundary layer) was $R = 0.75$.

3.1. Investigation of incorporating perpendicular viscosity

First we have compared the new model, based on the global ambipolarity constraint (Eq. (11), taking $\eta_\perp = (1/4)\eta_y$), with the old model based on the assumption that the plasma potential in the transition layer is defined by an exponentially decaying radial profile of $V_\perp$. We have done this for normal as well as inverted ($B_\phi \to -B_\phi$, $I_\mathrm{p} \to -I_\mathrm{p}$) magnetic field orientation. Results of this comparison are shown in Figs. 1–3. The new model strongly changes the radial electric field structure in the transition layer, which can be seen in Fig. 1 (shown at the bisectrix, just poloidally opposite to the ALT limiter). With the new model a very pronounced minimum of E_r develops close to the separatrix. This large negative value of E_r gives rise to a strong global plasma circulation in the transition layer close to the separatrix (Fig. 2). At outboard midplane we can also compare with experimentally measured values of V_x (Fig. 2(a)) [8]. For normal as well as for inverted field the experimental points show the same behaviour as the calculated velocities and confirm the abrupt velocity reversal when radially passing through the separatrix. The high velocity shear at the separatrix and the global circulation layer just inside the separatrix are clearly produced by the characteristic shape of the perpendicular drift velocity $V_\perp$ (Fig. 2(b)).

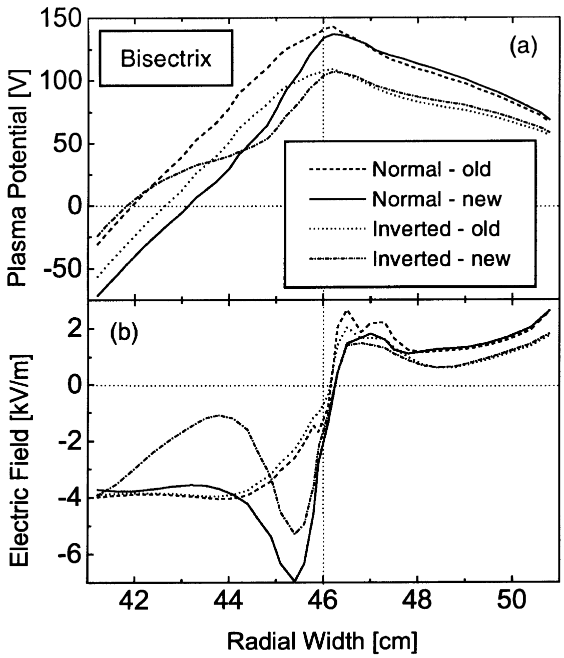

Fig. 1. Plasma potential (a) and electric field (b) at the bisectrix.

We have also plotted the poloidal dependence of the radial current j_r in the transition layer near the negative E_r spike (Fig. 3). Obviously the changes by the new model are confined to very narrow layers near the limiter sides. For the old model j_r is positive almost everywhere, hence global ambipolarity is violated. For the new model j_r becomes also locally negative, but the negative currents do not fully compensate the positive currents. We mention that also the density profiles near the limiter tips are affected by the new $\eta_\perp$-term in the Eq. (5) for the radial ion drift velocity.

Finally, in order to analyze the influence of $\eta_\perp = 1/4\eta_y$ on the radial electric field structure, we have made calculations for different perpendicular viscosities (all other parameters not changed). This is shown in Fig. 4. For increasing $\eta_\perp$ the negative spike of E_r is much more pronounced and consequently the electric potential slope much steeper. The concomitant velocity changes (Fig. 5(a) and (b)) are quite drastic. We remind that the factor 1/4 was taken from the classical viscosity

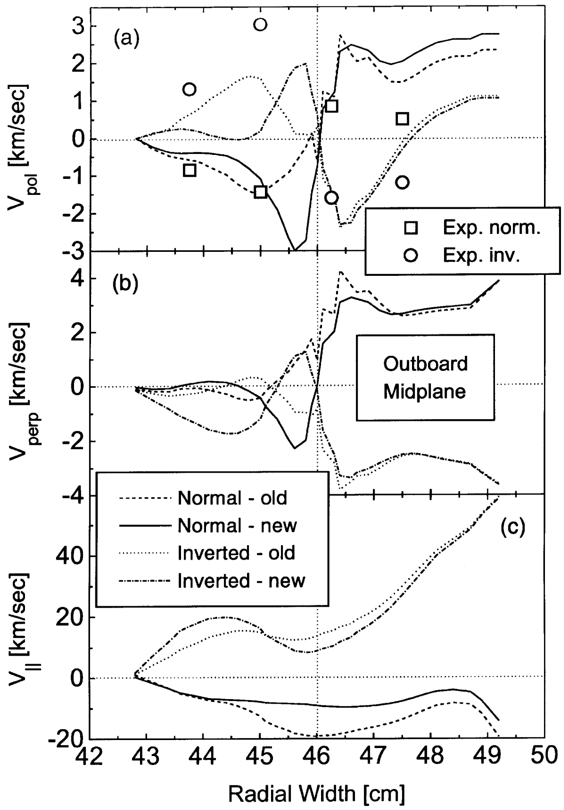

Fig. 2. Plasma velocities: poloidal (a), perpendicular (b), parallel (c), at outboard midplane (LFS). Experimental data scaled with factor 0.4.

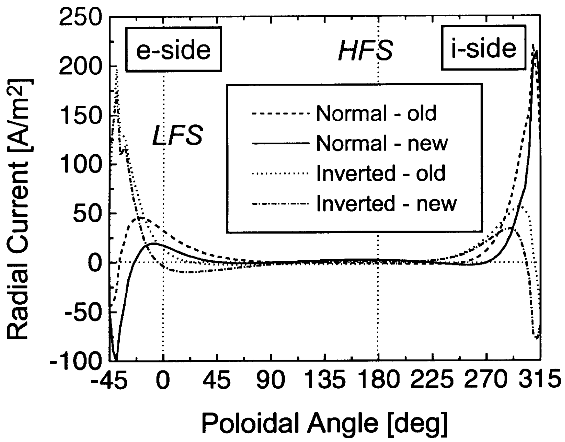

Fig. 3. Poloidal profiles of j_y in the transition layer at $r = 45.5$ cm.

coefficients [10], but there is no reason to assume that, when passing to anomalously enhanced values, the factor should remain the same.

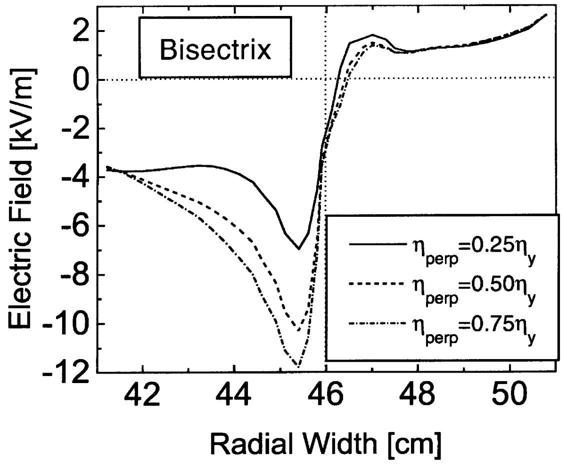

Fig. 4. Electric field at bisectrix for different $\eta_\perp$.

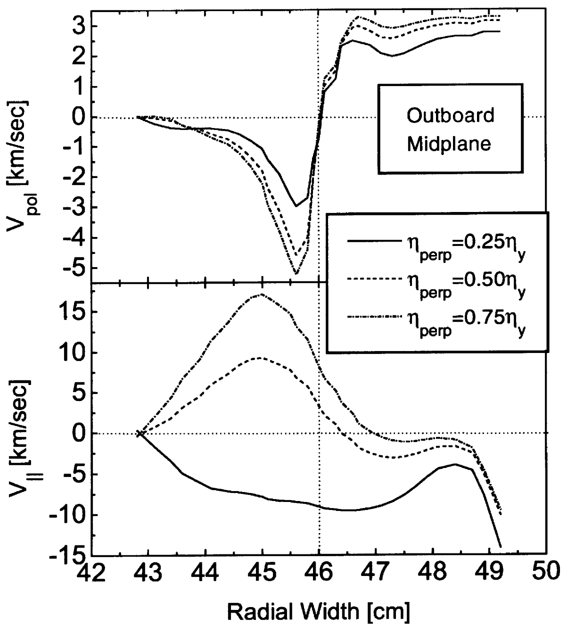

Fig. 5. Poloidal (a) and parallel (b) velocities at LFS for different $\eta_\perp$.

3.2. Conclusions

The inclusion of the perpendicular shear force enabled us to achieve global ambipolarity of the radial currents by properly adapting the perpendicular electric drift and hence the radial electric field and plasma potential in the transition layer. Whereas previously we had to assume ad hoc that the mean diamagnetic velocity decays exponentially to zero when going away from the separatrix, this assumption has now been replaced by a differential equation for $E_r = -\partial\Phi/h_y\partial y$ obtained from the global ambipolarity constraint. The perpendicular viscosity $\eta_\perp$ increases the order of the differential equation by one and thus allows to fulfil the boundary conditions. A major effect of the new model is that it induces a strong global plasma circulation in a layer of about 1 cm width, where the poloidal plasma velocity V_x goes all around the poloidal circumference. It is largely confirmed by experiment and directly connected to the negative spike of E_r just inside the separatrix, which is caused by the new $\eta_\perp$ term in the equations. Varying the ratio $\eta_\perp/\eta_y$ opens the possibility to model much better experimentally measured velocities by appropriately 'tuning' $\eta_\perp$ relative to η_y. However, we could not yet obtain perfect global ambipolarity, so in order to exploit the physics in the equations fully, further improvements to accuracy of the numerics are required.

Most interestingly in [5], where a divertor tokamak was modelled with a completely different numerical procedure, very similar profiles for the electric field and its negative spike were obtained (of order −8 kV/m in a layer of about 1 cm width). In the inverted case the minimum was less negative, which is also seen in our Fig. 1(b). Nevertheless this does not mean that the physical concept underlying the present model and that of [5] is the only one able to explain negative E_r-spikes. In [7] it is shown, that with a mainly neoclassical model incorporating a small anomalous diffusion (about 10% of ours) but introducing the so-called Burnett extension into the Braginskij viscosity tensor (including gyroviscosity), very similar radial E_r profiles as well as velocity profiles may be obtained in the narrow layer adjacent to the separatrix.

References

[1] R. Zagórski, H. Gerhauser, H.A. Claaßen, J. Nucl. Mater. 266–269 (1999) 1261.

[2] D. Reiser et al., in: Proceedings of the 26th Conference on Controlled Fusion and Plasma Physics, vol. 23J, Maastricht, Netherlands, ECA, 1999, p. 697.

[3] H. Gerhauser et al., Contrib. Plasma Phys. 40 (3&4) (2000) 309.

[4] R. Zagórski, H. Gerhauser, H.A. Claaßen, J. Techn. Phys. 40 (1) (1999) 99.

[5] T.D. Rognlien, G.D. Porter, D.D. Ryutov, J. Nucl. Mater. 266–269 (1999) 654.

[6] H.A. Claaßen, H. Gerhauser, Czech. J. Phys. 49 (Suppl. S3) (1999) 69.

[7] H.A. Claaßen, H.Gerhauser, Calculation of radial electric field, in: Proceedings of the 27th Conference on Controlled Fusion and Plasma Physics, Budapest, 2000, to be published.

[8] M. Lehnen et al., Investigations on density and temperature asymmetries, these Proceedings.

[9] H. Gerhauser, H.A. Claaßen, in: Proceedings of the 20th Conference on Controlled Fusion and Plasma Physics, vol. 17C, Pt. II, Lisbon, 1993, p. 835.

[10] S.I. Braginskij, Rev. Plasma Phys. 1 (1965) 205.

[11] H.A. Claaßen, H. Gerhauser, R.N. El-Sharif, Report of KFA Jülich, JÜL-2423 (January 1991).